~~DENTIAL~~

NAVORD REPORT 2277

THE EFFECT OF ALUMINUM ON UNDERWATER EXPLOSIVE PERFORMANCE: BUBBLE PULSE PARAMETERS FROM 1/LB CHARGES

1 January 1952

U. S. NAVAL ORDNANCE LABORATORY

WHITE OAK, MARYLAND

(6)

THE EFFECT OF ALUMINUM ON UNDERWATER EXPLOSIVE PERFORMANCE: BUBBLE PULSE PARAMETERS FROM 1-LB CHARGES,

by

(10) Ermine A. Christian, Jean A. Goertner,
J. P. Slifko [redacted] E. Swift, Jr.

(11) 1 Jan 52

(12) 35p.

Investigational group:

W. W. Hammack	J. E. Morgan, Jr.
C. E. Hopkins	Alys B. Russell
C. W. Mangold	B. W. Scott

ABSTRACT: Pressure-time recordings were made of the bubble pulses from 1-lb charges of RDX/TNT/Al mixtures. The percentage of aluminum was varied from 0 to 45%, with HBX-1 and HBX-3 compositions included. It was found that as aluminum content increases, the bubble pulse peak pressure and energy decrease, the positive duration increases, and the positive impulse remains relatively constant. Total bubble energy, as represented by the cube of the first bubble period constant, increases with increasing aluminum.

(17) NOL-Re2c-3-1

U. S. NAVAL ORDNANCE LABORATORY
WHITE OAK, MARYLAND

(250650)

Jm

NAVORD Report 2277 1 January 1952

The study reported here was carried out as a part of Task NOL-Re2c-3-1. This report is for information only and is not intended to be a basis for action. The accuracy of the results and the opinions expressed herein are the responsibility of the authors.

W. G. SCHINDLER
Rear Admiral, USN
Commander

Paul M. Fye

PAUL M. FYE
By direction

ACKNOWLEDGEMENTS

This program was undertaken as the result of a suggestion by Dr. Hans G. Snay, who also developed the method of base line adjustment used in evaluating the records. Mr. A. D. Yensen at White Oak and the Officers and personnel of NOU, Fort Monroe, Virginia were most cooperative in making necessary arrangements for use of facilities at NOU. Lt. John P. Kreckel, USN, and the crew of the EPCS 1413 did an outstanding job in spite of trying conditions at sea.

TABLE OF CONTENTS

		Page
I.	INTRODUCTION	1
II.	EXPERIMENTAL DETAILS	2
	Charges	2
	Rig and Instrumentation	2
III.	TREATMENT OF DATA	5
	Bubble Periods	5
	Bubble Pulse Parameters	10
IV.	DISCUSSION	13
APPENDIX A:	Base Line Adjustment	20
LIST OF REFERENCES		27
LIST OF FIGURES		
1.	Rig for 500-ft Depth Bubble Measurements	3
2.	Pressure-time Curves from Aluminized Explosives at 500 Foot Depth	6
3.	First Bubble Pulse Composite Plot for 0% Aluminum	11
4a.	Ratios of Period Constants Relative to Non-Aluminized Mixture for Equal Weight	14
4b.	Ratios of Successive Bubble Period Constants	14
5.	First Bubble Pulse Parameters Relative to Non-Aluminized Mixture for Equal Weight	16
6.	Total Bubble Energy Relative to HBX-1 for Equal Volume	18
7.	Period Constants Relative to HBX-1 for Equal Volume	19
8.	Parameters of First Bubble Pulse Relative to HBX-1 for Equal Volume	19

TABLE OF CONTENTS (Cont.)

		Page
LIST OF TABLES		
I.	Charge Specifications	2
II.	Measured Bubble Periods	8
III.	Bubble Period Constants	9
IV.	First Bubble Pulse Parameters	12
V.	Bubble Energies Relative to Non-Aluminized Mixture for Equal Weight	13
VI.	First Bubble Pulse Parameters. Ratios to Non-Aluminized Mixture for Equal Weight	15

THE EFFECT OF ALUMINUM ON UNDERWATER EXPLOSIVE PERFORMANCE: BUBBLE PULSE PARAMETERS FROM I-LB CHARGES

I INTRODUCTION

1. Recent explosion tests carried out against cylindrical models [a, b]*, and one shot against a submarine [c], have shown that the bubble pulse can be a major factor in hull-splitting attacks against submarines. However, exact knowledge as to the mechanism of such damage is at present lacking.

In order to study bubble pulse damage one should have a rather detailed knowledge of the bubble pulse itself - e.g., its peak pressure, positive impulse, energy and duration. Very little such information is available, and, furthermore, that suitable for controlled experiments is very scanty [d, e].

A recent study in this Laboratory [f] had indicated that bubble pulse damage was affected by the aluminum content of the explosive used. Consequently, this study of bubble pulse parameters as a function of aluminum content was initiated to discover if damage could be correlated with any particular parameter of the bubble pulse.

2. The explosives selected for study were RDX/TNT/aluminum mixtures with 5% wax desensitizer. The RDX/TNT ratio was fixed at 1.05/1.00 and amounts of aluminum up to 45% of the total weight were added. The percentages of aluminum were so chosen that both HBX-1 (17% aluminum) and HBX-3 (35% aluminum)** were included in this study. A few TNT charges were also included, for comparison with earlier results [d].

The tests reported here were fired at a depth of 500 feet in the ocean, and bubble pulse pressure-time recordings were made from forty-two charges. The shockwave parameters of these compositions were also studied from a second group of tests, and are discussed in reference [g].

---

* Such letters refer to the list of references at the end of this report.

** Actually, the RDX/TNT ratio in HBX-3 is 1.07/1.00 [h], but this difference is certainly negligible here.

II EXPERIMENTAL DETAILS

3. Charges. The charges, prepared by the Explosives Properties Division of this Laboratory, weighed 450 grams each, exclusive of booster, and were in the shape of cylinders with length roughly equal to diameter. Each charge was boostered at one end with 50 grams of pentolite. Compositions are shown in Table I, together with charge densities.

TABLE I

Charge Specifications

Composition, % by Weight				Density
Aluminum	RDX	TNT	Wax	gm/cc
0	48.6	46.4	5	1.61
10	43.5	41.5	5	1.66
17	40.0	38.0	5	1.69
25	35.9	34.1	5	1.72
35	30.7	29.3	5	1.79
45	25.6	24.4	5	1.83

4. Rig and Instrumentation. Four channels of electronic piezoelectric gauge recording equipment were used. These channels were similar to those used in previous shockwave recording [1], but had several important modifications in order to record the bubble pulses properly, since these phenomena are of relatively long duration and low pressure.

The gauge assembly and charge were held rigidly in a 17.5 ft diameter steel ring (Fig. 1). Steel cables of 1/8 in. size were used for positioning the gauges and cables; the charge was held by marlin. The charge axis was perpendicular to the plane of the ring so that all measurements were made off the side of the charge. The gauges were placed edge-on to the charge and outside the anticipated maximum bubble radius. The entire assembly was suspended by a 3/16 in. steel cable from the ship. Vanes on the sides of the ring prevented twisting of the cables.

The charge depths were found from the length of cable paid out. This method of measurement had been found

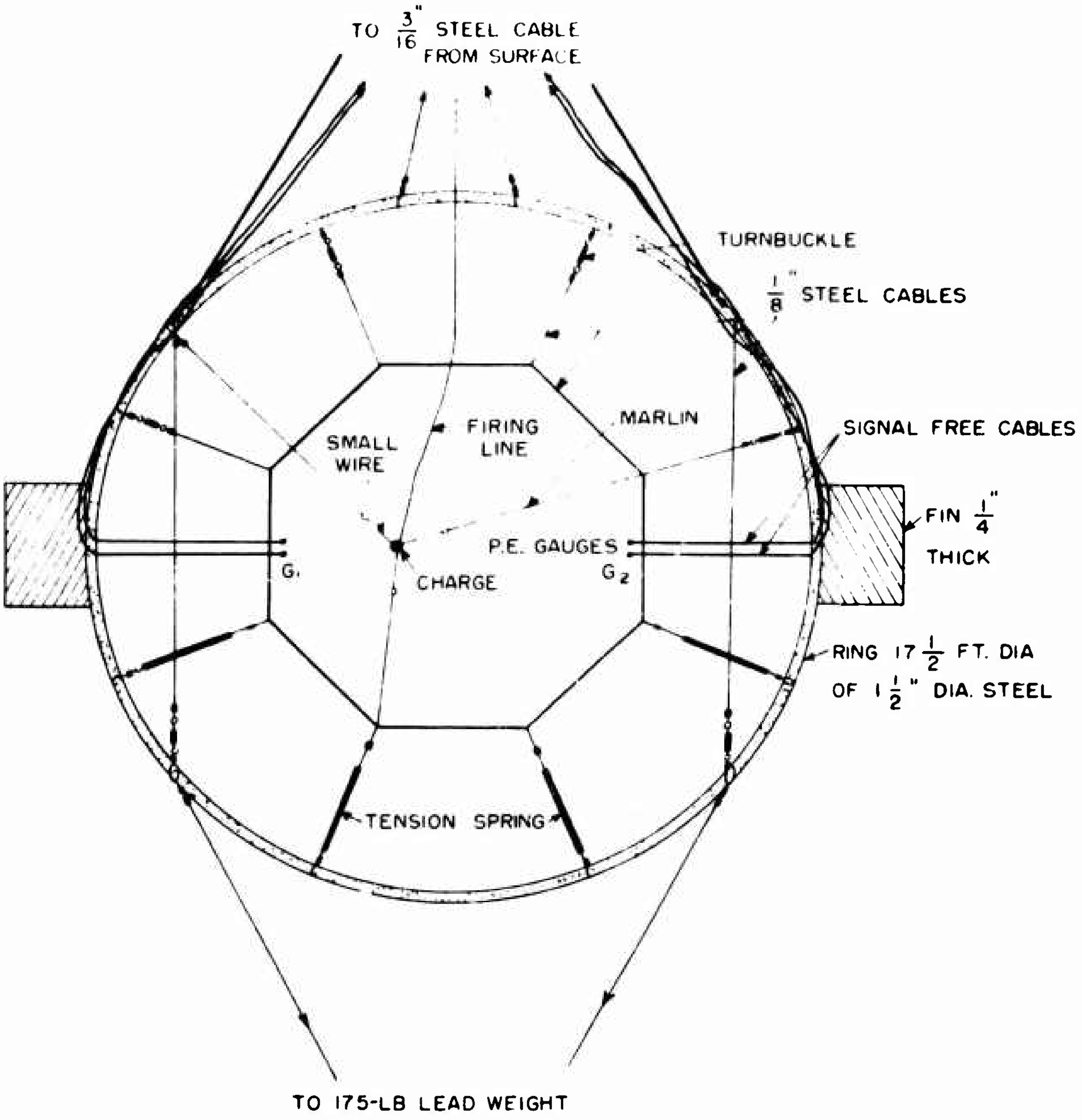

FIG. 1 RIG FOR 500-FT DEPTH BUBBLE MEASUREMENTS

satisfactory [d] whenever the ship's drift was small. Wire angles with the vertical were taken, but not used in the calculations*. A better check on the depths could have been provided by a pressure switch; however, the experimental pressure switch taken on the expedition proved faulty, so was not used.

5. Tourmaline four-pile gauges, 3/4 in. diameter, were used on all the measurements. This size is sufficiently sensitive (KA ~ 18 micromicrocoulombs/psi) to record the pressures expected. In view of the lack of need for high frequency response in bubble pulse measurements, such a large gauge size is permissible. The gauges were given three thin coatings of Zophar wax and dipped in clear Tygon paint. . Araldite 101 coating was also used on some gauges.

The gauges were soldered directly to 650-ft lengths of "signal-free" cable with polyethylene dielectric. The cables were terminated in a simple R-C series network [j] with R = 1.25 times the cable impedance and C = 2.0 times the cable capacity.

6. Cathode follower circuits with an input impedance of approximately 100 megohms were used on the outputs of the termination networks. This was found necessary in order to minimize low-frequency distortion, which is of importance in such bubble measurements. The modified DuMont 208 oscilloscopes [i] used in the measurements had an over-all low frequency time constant of about 1/2 second - probably adequate for these recordings.

In previous similar measurements [d], in which the same recording apparatus was used, an apparent negative shift of the base line after passage of the shockwave had been observed. This was believed to be due to grid current drawn by the extremely large shockwave signal. Hence a circuit was incorporated in the oscilloscopes to limit the shockwave signal to a reasonable value and thus prevent the base line shift. This circuit was installed in two of the four channels, one at each gauge distance, for comparison with the unmodified channels. Unfortunately, the limiting circuit did not eliminate the negative shift, and no real difference between the results from the two sets of channels was found.

---

* The cosine correction to the depth makes very little difference in the calculations, and is uncertain since the cable may not be straight. Actually, TNT period constants were closer to previous findings without it.

satisfactory [d] whenever the ship's drift was small. Wire angles with the vertical were taken, but not used in the calculations*. A better check on the depths could have been provided by a pressure switch; however, the experimental pressure switch taken on the expedition proved faulty, so was not used.

5. Tourmaline four-pile gauges, 3/4 in. diameter, were used on all the measurements. This size is sufficiently sensitive (KA ~ 18 micromicrocoulombs/psi) to record the pressures expected. In view of the lack of need for high frequency response in bubble pulse measurements, such a large gauge size is permissible. The gauges were given three thin coatings of Zophar wax and dipped in clear Tygon paint. An Araldite 101 coating was also used on some gauges.

The gauges were soldered directly to 650-ft lengths of "signal-free" cable with polyethylene dielectric. The cables were terminated in a simple R-C series network [j] with R = 1.25 times the cable impedance and C = 2.0 times the cable capacity.

6. Cathode follower circuits with an input impedance of approximately 100 megohms were used on the outputs of the termination networks. This was found necessary in order to minimize low-frequency distortion, which is of importance in such bubble measurements. The modified DuMont 208 oscilloscopes [i] used in the measurements had an over-all low frequency time constant of about 1/2 second - probably adequate for these recordings.

In previous similar measurements [d], in which the same recording apparatus was used, an apparent negative shift of the base line after passage of the shockwave had been observed. This was believed to be due to grid current drawn by the extremely large shockwave signal. Hence a circuit was incorporated in the oscilloscopes to limit the shockwave signal to a reasonable value and thus prevent the base line shift. This circuit was installed in two of the four channels, one at each gauge distance, for comparison with the unmodified channels. Unfortunately, the limiting circuit did not eliminate the negative shift, and no real difference between the results from the two sets of channels was found.

* The cosine correction to the depth makes very little difference in the calculations, and is uncertain since the cable may not be straight. Actually, TNT period constants were closer to previous findings without it.

While this base line effect was troublesome, it could be taken into account in the analysis of the results (see Appendix A). Ordinarily it amounted to about 40-60 psi; however, when a new gauge-cable combination was installed, the shift was considerably greater and decreased on successive shots with the same gauge and cable.

Timing was provided by a 1000 cycle tuning fork. Timing dots were obtained from a crater tube and recorded on the film simultaneously with the pressure record. The Selsyn camera drives and lucite camera drums [k] were driven at about 325 rpm, thus giving several bubble pulses on a 10 in. strip of film.

III TREATMENT OF DATA

Figure 2 shows tracings of pressure-time film records for three compositions. From continuous strip prints of the piezoelectric gauge records, measurements of the first three bubble periods and the pressure-time histories for the first bubble pulse were obtained.

7. Bubble Periods. The first three bubble period constants were calculated from the equation:

$$K_n = \frac{T_n Z_o^{5/6}}{W^{1/3}} \qquad n = 1, 2, 3$$

where:
K_n = period constant of n-th pulse
T^n = bubble period in sec
Z_o = absolute hydrostatic depth in ft of water (charge depth + atmospheric pressure in ft of water)
W = charge weight in lb

Since the booster has a different bubble energy than the main body of the charge, the directly measured period is that for a composite of two explosives. However, the weight of the booster, W_b, can be converted to an equivalent weight of base charge, W_x, by using successive approximations of the cubes of the first period constants [h], which are proportional to bubble energies:

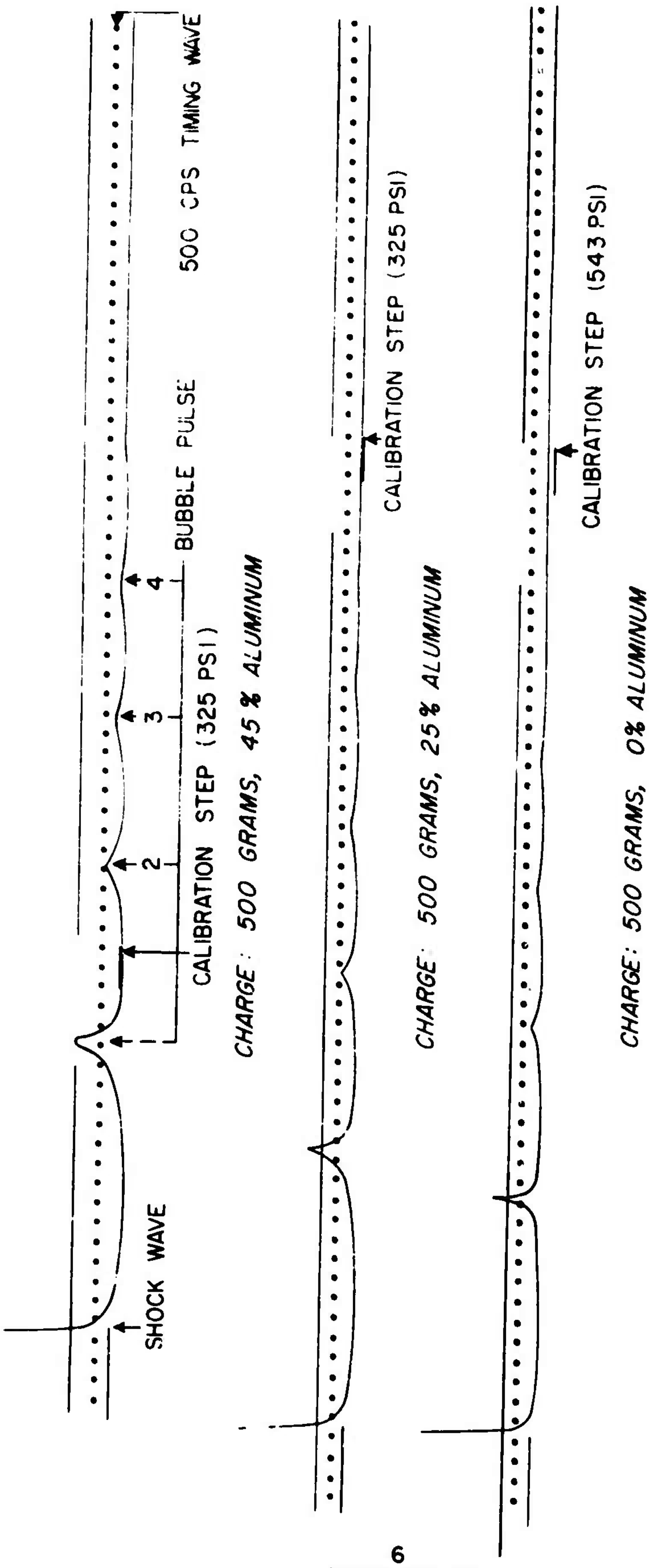

FIG. 2 PRESSURE-TIME CURVES FROM ALUMINIZED EXPLOSIVES AT 500 FOOT DEPTH

$$W_x = \left(\frac{K_b}{K_x}\right)_1^3 W_b$$

where:

x refers to base charge
b refers to booster

In the present series, a value of 4.35 [h] for the first period constant of the pentolite booster was used to calculate the corrected weights. The same corrected weight was used in calculating the second and third period constants.

8. The measured period values are given in Table II, and the average period constants, together with standard deviations, in Table III. There are few free water values in the literature with which to compare these results. Of the six compositions, only HBX-1 and HBX-3 have been reported. In reference [l] values for HBX-1 of 4.98, 5.22 and 5.14 were found at depths of 1, 2 and 3 miles using 1-lb charges. In reference [m] half-pound HBX-1 and HBX-3 charges were fired at 10, 79 and 115 ft. Assuming that the charges at 79 ft were sufficiently far away from interfering surfaces, the constants K_1 calculated by the method of paragraph 7 for the periods reported in [m] are 5.20 for HBX-1 and 5.70 for HBX-3.

TABLE II

MEASURED BUBBLE PERIODS

Composition (% Al)	Shot Number	Z_o (Ft Water)	T_1 (msec)	T_2 (msec)	T_3 (msec)
0	316	533	23.5	17.2	13.8
	322	534	24.3	17.9	14.7
	333	545	23.3	17.0	13.7
	339	545	23.1	16.9	13.7
	349	545	23.3	17.1	13.8
	350	545	23.1	17.0	13.7
	359	545	23.8	17.3	14.2
10	319	534	25.3	17.8	14.3
	320	534	25.3	17.9	14.3
	343	545	25.0	17.2	14.3
	361	545	25.1	17.5	14.2
	363	545	25.0	17.5	14.0
17	317	534	27.2	18.0	15.2
	326	545	26.6	17.8	14.6
	330	545	26.6	17.9	14.7
	340	545	26.5	17.7	14.7
	347	545	26.8	17.7	14.7
	352	545	26.4	17.8	14.7
	356	545	27.1	18.0	15.0
25	313	534	28.8	18.5	15.1
	324	545	28.3	18.2	14.8
	329	545	28.3	18.0	14.9
	338	545	28.1	18.0	14.9
	345	545	28.3	18.0	14.7
	351	545	28.3	18.2	14.9
	355	545	28.9	18.6	15.0
35	315	533	29.7	18.0	15.2
	325	545	29.1	18.3	14.9
	332	545	29.3	18.2	14.7
	341	545	29.1	17.8	14.9
	346	545	28.9	17.9	14.7
	354	545	29.2	18.2	15.0
	358	545	30.0	18.4	15.3

TABLE II (Cont.)

Composition (% Al)	Shot Number	Z_o (Ft Water)	T_1 (msec)	T_2 (msec)	T_3 (msec)
45	318	534	30.2	18.2	15.1
	321	534	30.6	18.4	15.0
	344	545	29.6	17.8	14.9
	360	545	29.8	18.0	14.9
	362	545	30.0	18.3	15.1
(TNT)	327	545	23.0	16.2	13.4
	328	545	22.4	15.8	13.1
	337	545	22.1	15.5	13.0

TABLE III

BUBBLE PERIOD CONSTANTS

Composition (% Al)	K_1	σ_{m_1}	K_2	σ_{m_2}	K_3	σ_{m_3}	Average Corrected Weight* (pounds)
0	4.30	±0.52%	3.14	±0.51%	2.56	±0.88%	1.11
10	4.62	±0.20%	3.22	±0.46%	2.61	±0.54%	1.09
17	4.97	±0.24%	3.31	±0.34%	2.75	±0.27%	1.07
25	5.31	±0.32%	3.41	±0.45%	2.79	±0.27%	1.06
35	5.48	±0.47%	3.37	±0.81%	2.80	±0.59%	1.05
45	5.59	±0.27%	3.38	±0.46%	2.79	±0.53%	1.05
(TNT)	4.22	±0.70%	2.97	±0.81%	2.47	±0.50%	1.03

* See Paragraph 7

9. Bubble Pulse Parameters. Measurements on the first bubble pulse of the various compositions were made from composite pressure-time curves drawn from the records for each of the two gauge positions. It was impossible to make these measurements using a set of pressure and time axes with origin at the point of the shockwave discontinuity; due to anomalous responses of the recording mechanism (see paragraph 6), a simple extension of the shockwave hydrostatic pressure line of each record did not provide a reasonable base line for bubble pulse measurements.

Composite plots were obtained from the individual records by first adjusting the maximum pressure of each pulse to the same time and then locating the first minimum pressure point of each record at the same pressure level. The time location of these minimum pressure values was not necessarily the same. A smoothed curve was drawn through the points, and a base line was determined in the manner described in Appendix A*. Figure 3 shows such a composite curve from 14 records. In Fig. 3 are indicated the final adjusted base line, the locations of several minimum pressure points, and the half-periods used as limits of integration. The half-period values are averages of the various periods (Table II).

10. The following bubble pulse parameters were measured from the composite plots:

1) ΔP_m - maximum positive pressure deflection above hydrostatic
2) Δt - duration of the positive portion of the pulse
3) $I = \int p\,dt$ - positive impulse; integrated over Δt
4) $E = \int p^2 dt$ - "energy"; integrated over the interval from the mid-point of the first bubble period to the mid-point of the second bubble period**

Integrations were performed with a moment planimeter.

Values of these parameters measured with the arbitrary base line are given in Table IV. A comparison with earlier work on TNT is given in Appendix A.

* This arbitrary base line should correspond to the hydrostatic pressure.

** Energy flux as defined by $\frac{1}{\rho_o c_o} \int p^2 dt$ is not reported.

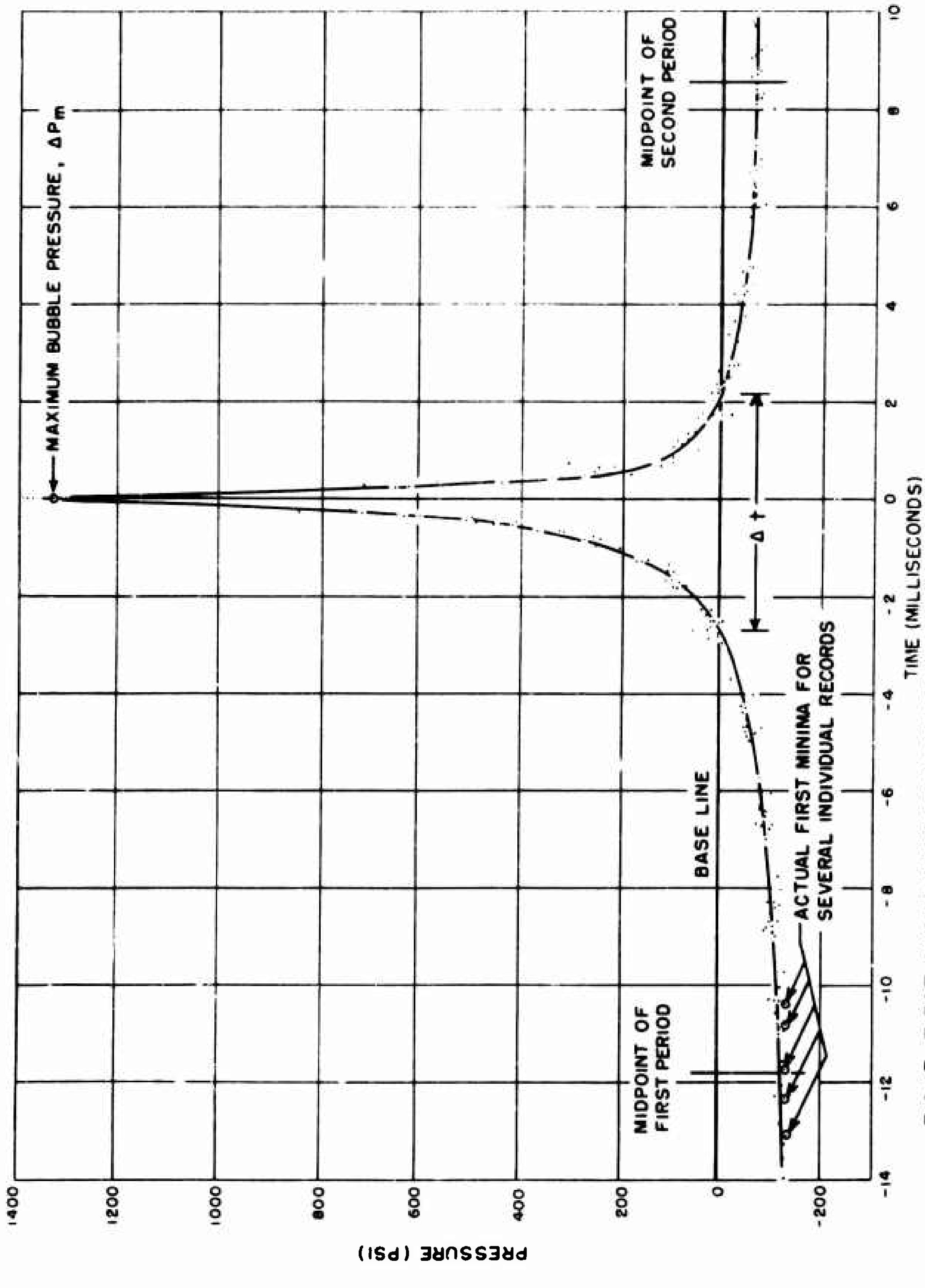

FIG. 3 FIRST BUBBLE PULSE COMPOSITE PLOT FOR 0 % ALUMINUM, R = 35 INCHES

TABLE IV

FIRST BUBBLE PULSE PARAMETERS

Composition (% Al)	Number of Charges	Charge-to-Gauge Distance = 35 in.				Charge-to-Gauge Distance = 70 in.			
		ΔP_m (psi)	Δt* (msec)	$\int p\,dt$* (psi-sec)	$\int p^2 dt$* (psi^2-sec)	ΔP_m (psi)	Δt* (msec)	$\int p\,dt$* (psi-sec)	$\int p^2 dt$* (psi^2-sec)
0	7	1320	4.82	1.16	890	680	5.18	0.56	220
10	5	1250	5.52	1.23	905	620	4.94	0.68	250
17	7	1110	5.62	1.32	840	570	5.65	0.68	235
25	7	900	6.07	1.31	730	465	6.39	0.70	215
35	7	710	6.64	1.36	680	350	6.86	0.69	175
45	5	535	7.26	1.34	600	270	6.86	0.68	140
(TNT)	3	1120	4.59	1.09	710	545	4.93	0.51	160

* Δt = Duration of positive portion of bubble pulse

$\int p\,dt$ = Positive impulse; integrated over Δt

$\int p^2 dt = \int_{T_1/2}^{T_2/2} p^2 dt$ where T_1 and T_2 are first and second bubble periods respectively

IV DISCUSSION

11. The various bubble parameters obtained were tabulated as values for the aluminized explosives relative to the corresponding values for the non-aluminized explosive. The relative total bubble energy of each mixture was expressed as the cube of its first period constant divided by the cube of the first period constant of the non-aluminized mixture. The bubble energy ratios on an equal weight basis are given in Table V for the first three periods.

TABLE V

BUBBLE ENERGIES RELATIVE TO NON-ALUMINIZED MIXTURE FOR EQUAL WEIGHT

% Al	First Period $(K_x/K_0)^3$	Second Period $(K_x/K_0)^3$	Third Period $(K_x/K_0)^3$
0	1.00	1.00	1.00
10	1.24	1.08	1.06
17	1.55	1.17	1.24
25	1.88	1.28	1.30
35	2.08	1.24	1.31
45	2.20	1.25	1.30

The values obtained are plotted against aluminum content in Fig. 4. From Fig. 4.a it is seen that the total bubble energy (i.e. that for the first period) increases markedly with aluminum content. Although it is not evident here, previous work [h] indicates that the bubble energy has a broad maximum around 45% aluminum. Bubble energies for the second and third periods are seen to be less strongly affected by an increase in aluminum content.

Fig. 4.b shows that the energy in the second bubble period becomes a smaller fraction of that in the first as the aluminum content is increased. This indicates that the energy losses between the first and second periods must become greater as the aluminum content is increased. However, the energy losses between the second and third period are little affected by aluminum content.

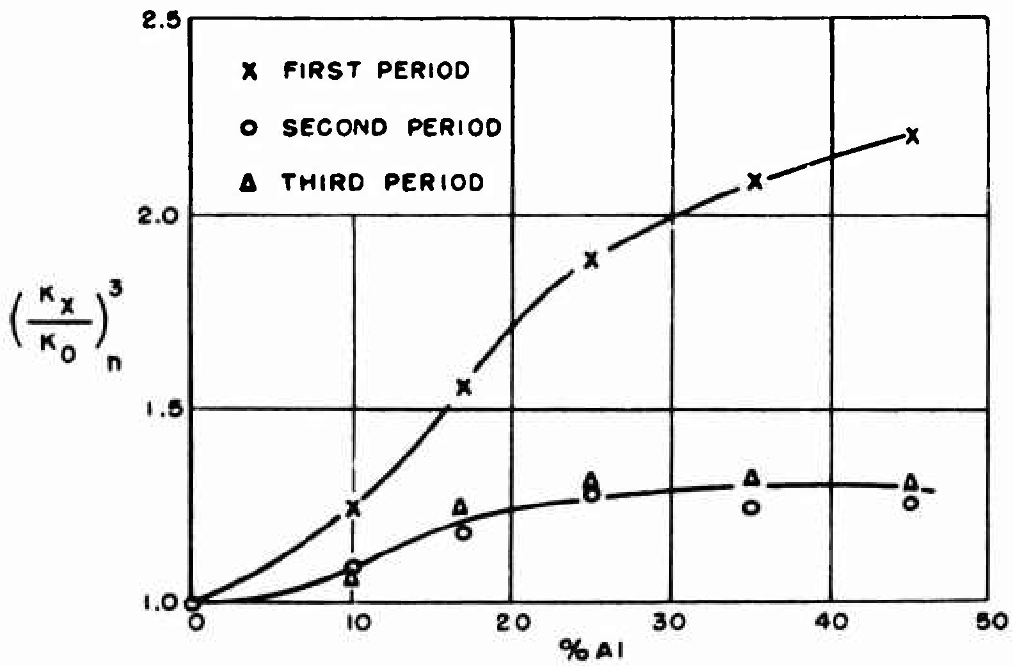

FIG 4a RATIOS OF PERIOD CONSTANTS RELATIVE TO NON-ALUMINIZED MIXTURE FOR EQUAL WEIGHT

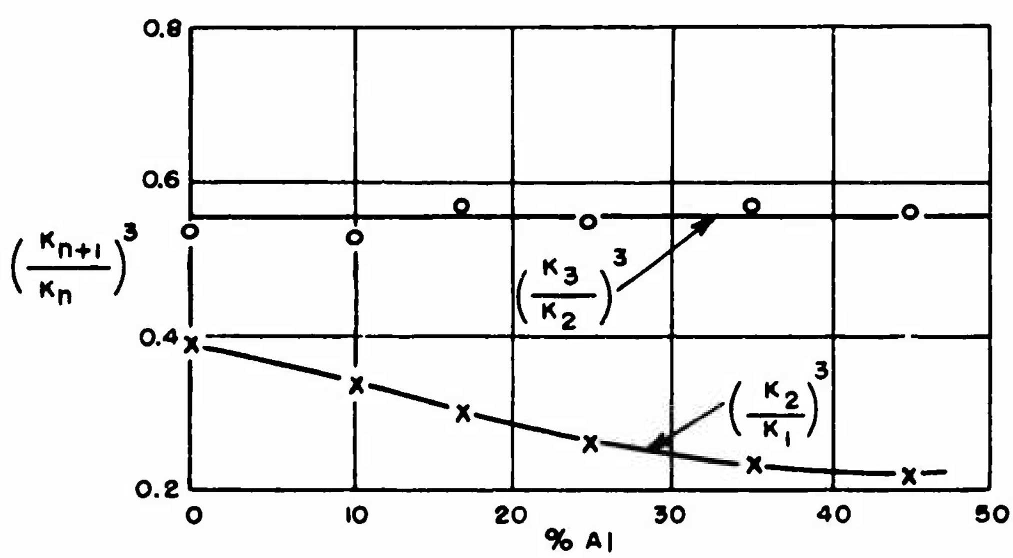

FIG. 4b RATIOS OF SUCCESSIVE BUBBLE PERIOD CONSTANTS

12. The relative values of the first bubble pulse parameters for equal charge weights are given in Table VI. Values for both the 35 in. and the 70 in. distance are given. These ratios for the 35 in. distance are plotted against aluminum content in Fig. 5. The curves for the 70 in. distance are essentially the same, except that the energy curve lies about 10% higher at the first three points, showing a maximum at 10% aluminum. In fact, there was so little variation with distance that the pressure-time histories at 35 in. and 70 in. can be practically superimposed on a non-dimensional plot of $p/\Delta P_m$ vs $t/\Delta t$.

Both the impulse and positive duration increase with aluminum content, the impulse levelling off to a broad maximum. The maximum pressure of the pulse decreases steadily with aluminum content and so does the energy. It is difficult to reconcile this trend with the increasing loss of energy with aluminum content found between the first and second periods, as noted in paragraph 11.

13. The above presentation of results relative to an equal weight of the non-aluminized explosive, while it shows clearly the effect of aluminum content, does not directly show the significance of this effect in terms of a standard explosive used in service weapons of given volume. In Figs. 6, 7 and 8 the results of these tests, along with some previously reported data, are shown relative to HBX-1 for equal volumes of explosive. The relative values at the 35% aluminum point represent HBX-3/HBX-1 on an equal volume basis.

TABLE VI

FIRST BUBBLE PULSE PARAMETERS
RATIOS TO NON-ALUMINIZED MIXTURE FOR EQUAL WEIGHT

Composition	Charge-to-Gauge Distance = 35 inches				Charge-to-Gauge Distance = 70 inches			
(% Al)	ΔP_m	Δt^*	$\int pdt^*$	$\int p^2dt^*$	ΔP_m	Δt^*	$\int pdt^*$	$\int p^2dt^*$
0	1.00	1.00	1.00	1.00	1.00	1.00	1.00	1.00
10	0.95	1.15	1.06	1.02	0.92	0.95	1.17	1.13
17	0.84	1.17	1.14	0.95	0.84	1.09	1.16	1.07
25	0.68	1.26	1.13	0.82	0.68	1.23	1.20	0.98
35	0.54	1.38	1.18	0.77	0.52	1.33	1.18	0.79
45	0.4[illegible]	1.51	1.16	0.68	0.40	1.33	1.16	0.63

* See Table IV

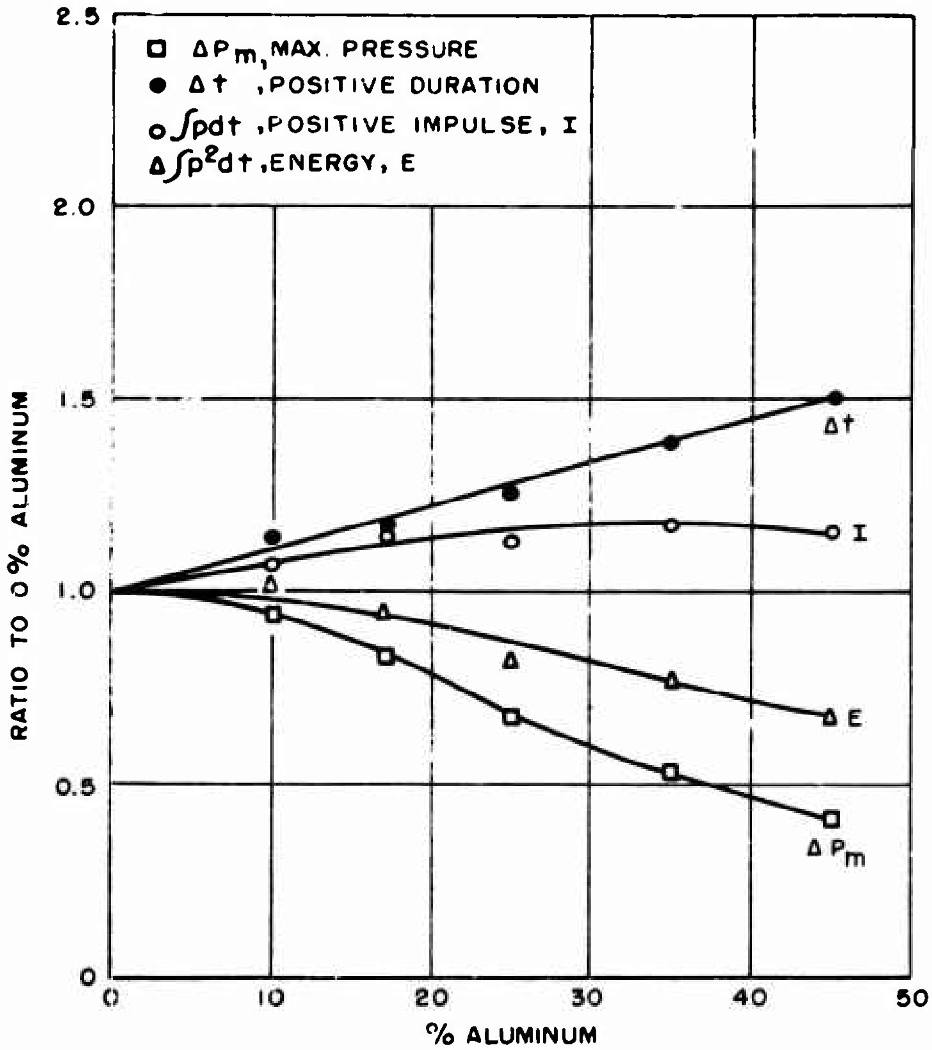

FIG. 5 FIRST BUBBLE PULSE PARAMETERS RELATIVE TO NON-ALUMINIZED MIXTURE FOR EQUAL WEIGHT

(CHARGE-TO-GAUGE DISTANCE = 35 INCHES)

In Fig. 6 are shown the total bubble energy ratios from the present free-water tests, and the shallow-water tests of references [h] and [g]. The free-water values (solid line) are slightly different from the shallow-water results which must be corrected for surface and bottom effects. The shallow-water measurements of these identical charges [g] are in excellent agreement with previous results (dotted line) where a large variety of RDX/TNT/Al mixtures was tested under similar conditions [h]. In Fig. 6, the values shown for the HBX-3/HBX-1 bubble energy ratio are 1.42 for free water, and 1.36 for shallow water shots. In addition, there are reported values of 1.50 for 13-pound charges in free water [n], and 1.35 [m] and 1.41 [o] for half-pound charges in shallow water.

14. For Figs. 7 (ratios of period constants) and 8 (bubble pulse parameters) the values of Figs. 4 and 5 were recomputed relative to HBX-1, and converted to an equal volume basis by means of density ratios of the explosives. For Fig. 8, the parameters of the first bubble pulse were obtained on an equal volume basis by assuming the acoustic relationships: ΔP_m proportional to $W^{1/3}$, I proportional to $W^{2/3}$ and E proportional to W. The ratios of Δt are not shown.

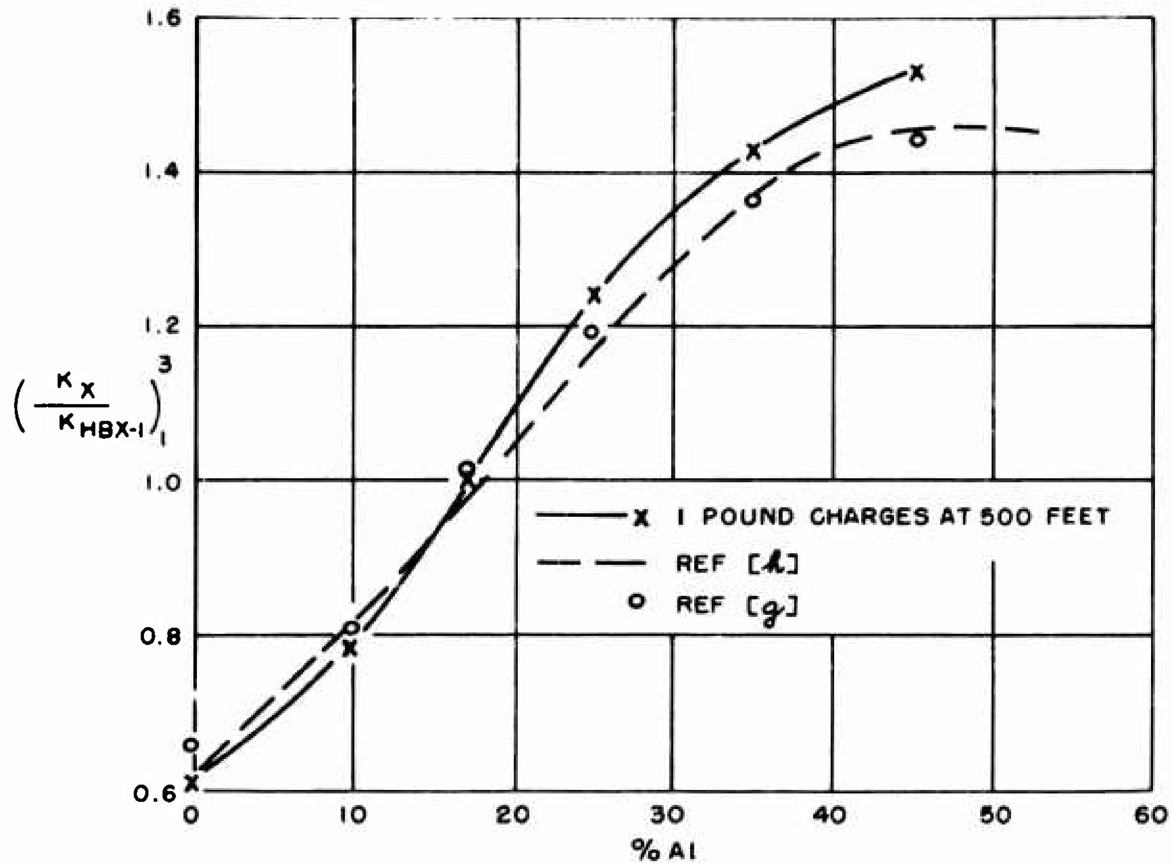

FIG. 6 TOTAL BUBBLE ENERGY RELATIVE TO HBX-1 FOR EQUAL VOLUME

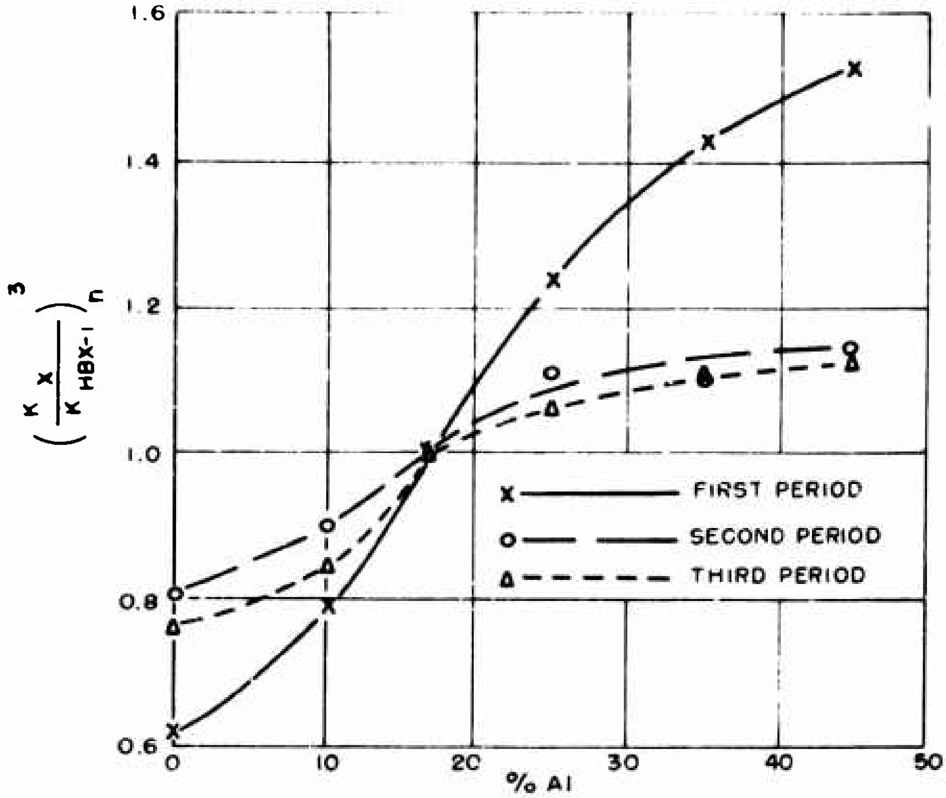

FIG. 7 RATIOS OF PERIOD CONSTANTS RELATIVE TO HBX-1 FOR EQUAL VOLUME

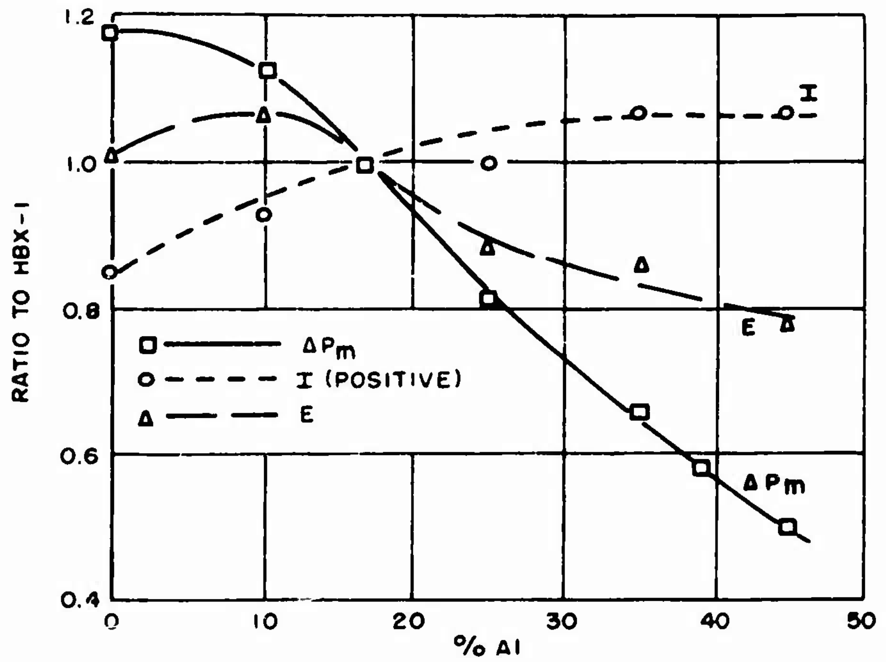

FIG.8 PARAMETERS OF FIRST BUBBLE PULSE RELATIVE TO HBX-1 FOR EQUAL VOLUME
(CHARGE-TO-GAUGE DISTANCE = 35 INCHES)

APPENDIX A

For measurements of bubble pulse parameters, the base line was so located that the minimum pressure value was equal to a calculated minimum pressure ΔP_M*.

As a first approximation, ΔP_M was calculated as in reference [d], where the same problem was encountered. Because of the difference in explosive composition, equation [A-27] in [d] was modified for use here with the assumptions: (a) that the relative bubble energy of two explosives is proportional to the cube of the ratio of their period constants, and (b) that the adiabatic parameters γ and k for the explosives considered do not vary radically from those for TNT. On the basis of these assumptions, the equation for the first minimum pressure becomes:

$$\Delta P_M = -5.16 \left(\frac{K_x}{K_{TNT}}\right) Z_o^{2/3} \frac{W^{1/3}}{R} \qquad (1)$$

where:

K = first bubble period constant

Z_o = absolute hydrostatic depth in ft of water (charge depth + atmospheric pressure in ft of water)

R = charge-to-gauge distance in ft

W = charge weight in lb

x refers to explosive other than TNT

---

* In this discussion the usual notation for maximum and minimum bubble pressures will be used:

ΔP_M = pressure at maximum bubble radius (minimum pressure)

ΔP_m = pressure at minimum bubble radius (maximum pressure)

If this method were applicable to the explosives studied here, the difference between the observed minimum pressure (measured from the recorded hydrostatic line) and the calculated ΔP_M should be the same order of magnitude regardless of composition. Since, however, these differences consistently decreased with increasing percentage of aluminum, equation (1) was considered inadequate.

A more general approach which utilizes an easily measured quantity, the recorded total deflection ($\Delta P_m - \Delta P_M$), was therefore used for determining the calculated minimum pressure. This method was derived from the following equations [p]:

$$\Delta P_M = - \frac{P_o L}{R} \left[a_M - \frac{(\gamma-1)k}{a_M \, 3\gamma-1} \right] \tag{2}$$

$$\Delta P_m = \frac{P_o L}{R} \frac{(\gamma-1)}{k^{2/3(\gamma-1)}} \left[1 - \frac{k^{1/(\gamma-1)}}{\gamma-1} \right] \tag{3}$$

where:

ΔP_M = minimum bubble pressure
ΔP_m = maximum bubble pressure
P_o = absolute hydrostatic pressure in lb/in.^{2}
R = charge-to-gauge distance in ft
L = scale factor for length, as given in [p]
a_M = non-dimensional maximum bubble radius

The actual maximum radius, A_M, is given by:

$$A_M = La_M \tag{4}$$

Using (4):

$$\Delta P_M = -\frac{P_o}{R} A_M \psi_1 \quad (5)$$

$$\Delta P_m = \frac{P_o}{R} A_M \psi_2 \quad (6)$$

where:

$$\psi_1 = 1 - \frac{(\delta-1)k}{a_M^{3\delta}} \quad (7)$$

$$\psi_2 = \frac{\delta-1}{a_M k^{2/3(\delta-1)}} \left[1 - \frac{k^{1/(\delta-1)}}{\delta-1}\right] \quad (8)$$

From (5) and (6):

$$\Delta P_m - \Delta P_M = \frac{P_o}{R} A_M \psi_3 \quad (9)$$

where:

$$\psi_3 = \psi_1 + \psi_2$$

The maximum radius A_M, in feet, is given by (4) in which:

$$L = 8.64 \left(\frac{2 P_o}{3\rho}\right)^{1/2} \frac{T}{t}$$ (Equations (9.3) and (9.5), reference [q]).

where:

P_o = absolute hydrostatic pressure in lb/in.^{2}
ρ = water density in gm/cc
T = actual time in seconds
t = non-dimensional time

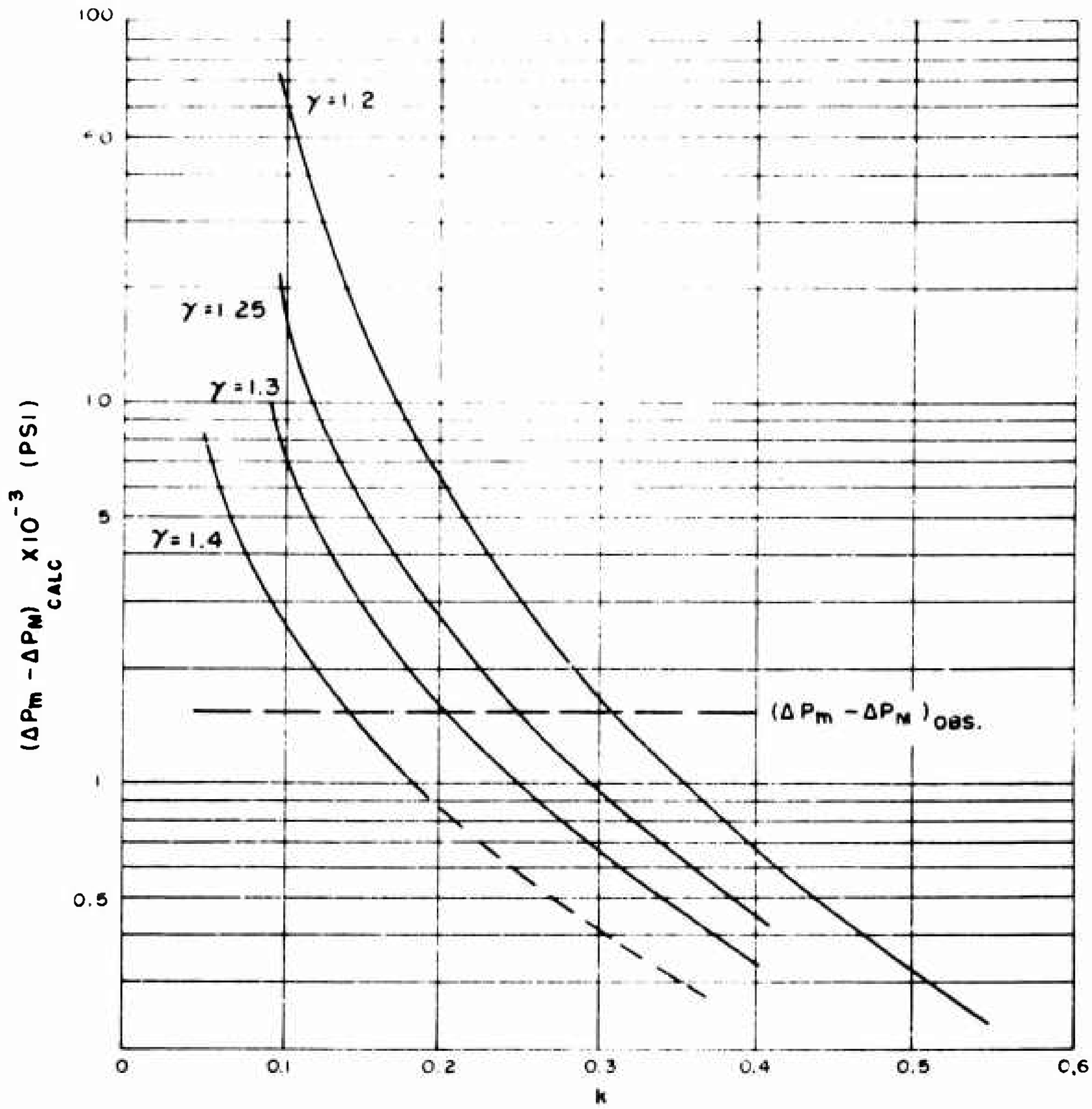

FIG. A-1 $(\Delta P_m - \Delta P_M)_{calc.}$ VS k

NON-ALUMINIZED MIXTURE AT 35 INCHES

(FIRST TOTAL DEFLECTION)

Using the values for a_M and t from [q] and [r], the quantity $(\Delta P_m - \Delta P_M)$ was calculated and plotted as a function of γ and k for one composition at one distance. Figure A-1 shows such a plot for the non-aluminized composition at the 35 inch distance for the first total deflection $(\Delta P_m - \Delta P_M)_1$. The values of observed $(\Delta P_m - \Delta P_M)$ were measured from pressure minimum to succeeding pressure maximum without regard to any base line. With the values of k and γ for which $(\Delta P_m - \Delta P_M)_{calc.} = (\Delta P_m - \Delta P_M)_{obs.}$ [see Fig. A-1], several values of ΔP_M may be calculated from (5) and plotted as a function of γ; Fig. A-2 shows such a plot for the same composition and distance as Fig. A-1.

FIGURE A-2. CALCULATED ΔP_{M_1} vs γ

0% Aluminum Distance = 35 inches
Temperature = 300° K

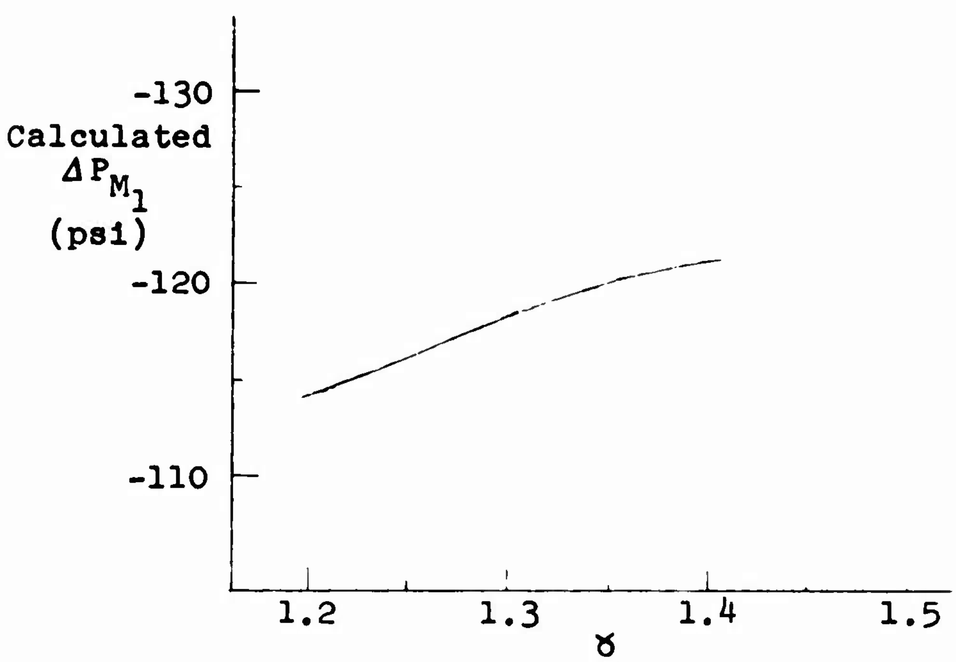

In order to obtain a calculated ΔP_M, a suitable value of γ for each explosive composition was determined in the following manner:

$$\gamma = 1 + \frac{Rn_g}{\Sigma n_i c_{v_i}} \tag{10}$$

where:

R = gas constant = 1.986 cal/°C mole

n_g = number of gaseous moles of decomposition products

i refers to the components of the decomposition product (H_2O, CO, etc.)

n_i = number of moles of i

c_{v_i} = molar heat capacity of the i-th component [s]

The values of γ were calculated for a temperature of 300 °K. The decomposition products used were those of the "CO arbitrary decomposition equation" for aluminized and those of the "H_2O arbitrary decomposition equation" for non-aluminized explosives [t].

The above method of calculating minimum pressures was applied to both the first and second bubble maxima (ΔP_{M_1} and ΔP_{M_2}) in order to determine two points on the base line. A straight line connecting these two pressure points was, in every case, below and very nearly parallel to the recorded hydrostatic pressure line.

Further slight adjustments of the calculated base line were made in such a way that the net value of $\int p dt$ between successive bubble maxima was zero [u]. The times of the first and second bubble maxima were taken to be the first and second half-periods, respectively. The necessary adjustments were of the order of five to fifteen lb/in^2. and were made parallel to the calculated base line.

In order to compare the above method of base line setting with that presented in [d], results obtained for ΔP_m, impulse, and energy for TNT by the two methods are shown in Table A-I. An approximate value of 5.6 for $\rho_o c_o$ for the present series was used.

TABLE A-I

	$\frac{W^{1/3}}{R}$	ΔP_m	$\frac{\int p dt}{W^{1/3}}$ (Impulse)	$\frac{\int p^2 dt}{\rho_o c_o W^{1/3}}$ (Energy)	First Period Constant
Present Series	0.356	1119	1.081	125	4.22
Reference [d]	0.352	1140 - 1210	1.12 - 1.17	134 - 141	4.31

The values for pressure, impulse, energy and period constant are consistently lower for the present TNT measurements than those obtained in reference [d], which might be due to a slight difference in charge weight or density. If both sets of data are adjusted to the same pressure and time scale (given by ΔP_m and period constant) the values for momentum and energy appear to be almost identical.

LIST OF REFERENCES

[a] "Damage to Thin Steel Cylindrical Shells by Underwater Explosions, III". J. C. Decius and W. S. Shultz. NAVORD 404, 11 September 1947.

[b] "Damage Mechanism of 1/8 Scale Submarine Pressure Models Under Explosive Loading". A. H. Keil. U.E.R.D. Report 7-50, October 1950.

[c] "Report of Two Experimental Depth Charge Attacks Against the German Submarine U-1105". H. G. Snay and E. Swift, Jr. NOLM 10573, 1 July 1950.

[d] "Measurement of Bubble Pulse Phenomena IV: Pressure-Time Measurements in Free Water". A. B. Arons, J. P. Slifko, A. H. Carter, D. R. Yennie and C. L. Wingate. NAVORD 408, 6 November 1947.

[e] "Phenomena Associated with the Pulsations of the Gas Globe Produced by Underwater Explosions of Small Charges". Avis Borden, A. B. Arons, and B. Stiller. DTMB Report C-232, July 1949.

[f] "Damage to Small Cylinders of Different Thicknesses by Underwater Explosions". L. Glickman and H. G. Snay. NOLM 10595, 14 December 1949.

[g] "The Effect of Aluminum on Underwater Explosive Performance: Shockwave Parameters from 1-lb Charges". R. W. Astheimer, Ermine A. Christian and E. Swift, Jr. NAVORD 2317. In publication.

[h] "Comparisons of the Underwater Power of Explosives in the RDX/TNT/Aluminum System Using Small Charges". C. R. Niffenegger and E. Swift, Jr. NAVORD 2105, 25 June 1951.

[i] "Electrical Instruments for Study of Underwater Explosions and Other Transient Phenomena". R. H. Cole, David Stacey and R. M. Brown. NDRC Report A-360, OSRD Report 6238, November, 1945.

[j] "A Study of Piezoelectric Gauge Cable Termination". Otto Meier, Jr. NOLM 10467, 14 November 1947.

[k] "Explosion Studies at Depths Greater than One Mile in the Ocean. IV. Instrumentation". R. S. Price, J. P. Slifko. NOLM 10893, 1 June 1950.

LIST OF REFERENCES (Cont.)

[l] "Studies of Explosions at Depths Greater than One Mile in the Ocean. VI. Bubble Period Measurements". J. P. Slifko. NAVORD 2276. In publication.

[m] "Effectiveness of HBX-1 and HBX-3 Against Submarine Models". H. M. Schauer. U.E.R.D. Report 8-51, May 1951.

[n] "Whipping Response of Submerged Cylinders as Caused by Different Explosives". A. H. Keil. U.E.R.D. Report 11-51, October 1951.

[o] "A Comparison of Different Boosters for Half-Pound HBX-1 and HBX-3 Charges". C. R[illegible]fenegger and J. P. Slifko. NAVORD 1748, 9 Ja[illegible]y 1951.

[p] "Secondary Pressure Pulses Due to Gas Globe Oscillation in Underwater Explosions II: Selection of Adiabatic Parameters in the Theory of Oscillation". A. B. Arons. NAVORD 420, 1 May 1948.

[q] "Measurement of Bubble Pulse Phenomena, III. Radius and Period Studies". E. Swift, Jr. and J. C. Decius. NAVORD 97-46, 11 September 1947.

[r] "Theory of Underwater Explosion Bubbles". Bernard Friedman. Institute for Mathematics and Mechanics, N. Y. University. Report No. IMM-NYU 166, September 1947.

[s] "Contributions to the Data on Theoretical Metallurgy X: High Temperature Heat Content, Heat Capacity and Entropy Data for Inorganic Compounds". K. K. Kelly, U. S. Department of the Interior, Bureau of Mines, Bulletin 476.

[t] "Analysis of Experimental Data on Detonation Velocities". E. A. Christian and H. G. Snay. NAVORD 1508, 1 February 1951.

[u] "Energy Partition in Underwater Explosion Phenomena". A. B. Arons and D. R. Yennie. NAVORD 406, 1 October 1947.